HOSTED BY

ELSEVIER

CrossMark

Available online at www.sciencedirect.com

ScienceDirect

Journal of Magnesium and Alloys 3 (2015) 106−111
www.elsevier.com/journals/journal-of-magnesium-and-alloys/2213-9567

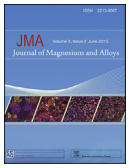

Full length article

Effect of temperature on the mechanical abnormity of the quasicrystal reinforced Mg−4%Li−6%Zn−1.2%Y alloy

C.Q. Li [a,b], D.K. Xu [a,*], T.T. Zu [a], E.H. Han [a], L. Wang [b]

[a] *Environmental Corrosion Center, Institute of Metal Research, Chinese Academy of Sciences, Shenyang 110016, China*
[b] *School of Materials and Metallurgy, Northeastern University, Shenyang 110819, China*

Received 22 September 2014; revised 27 January 2015; accepted 2 February 2015
Available online 17 April 2015

Abstract

The serrated phenomena of the quasicrystalline phase reinforced Mg−4%Li−6%Zn−1.2%Y alloy after the extrusion, solid solution treatment and aged treatment have been investigated at different temperatures. The result shows that when the temperature is above 100 °C, the serrated phenomenon becomes weak and all the serrated amplitudes are lower than 1 MPa. Among them, the serrated amplitude of samples in aged condition is the lowest and the value is only 0.1−0.2 MPa. The underneath mechanism for the lower plastic instability at higher temperature (≥100 °C) can be ascribed to the weak pining effect of solute atoms on the movement of dislocation and release of the pile-up dislocations.

Keywords: Mg−Li; PLC; Quasicrystal; High temperature deformation; Mechanical property

1. Introduction

Being as the lightest engineering and structural metallic materials, Mg−Li alloys have obtained great interest from the aerospace and automobile industries [1−4]. However, their applications as the engineering and structural components were limited to some extent due to the low strength, weak work hardening and poor corrosion resistance [5,6]. To solve these issues, researchers have tried different strengthening methods especially the alloying methods, such as the additions of Al, Ca, Zn, RE and so on [7−9]. Among them, by adding Zn and Y and controlling Zn/Y atomic ratio in Mg−Li alloys, I-phase (Mg_3Zn_6Y, icosahedral quasicrystal structure) could be formed and greatly improve their mechanical properties and corrosion resistance [9−11].

Besides the issues mentioned above, the plastic instability (i.e. occurrence of the serrated flow during tensile or compressive testing) is another problem and can easily occurred in Mg−Li alloys [4,12,13]. So far, the serrated flow represented in the time domain was called as Portevin-Le Chatelier (PLC) effect and has been widely investigated [14−21]. Recently, it has been reported that the occurrence of plastic instability of Mg−Li alloy were related to the applied strain rate range [15,16,19]. In addition, Hu et al. reported that the precipitation can significantly influence the PLC effect of Mg alloys [18]. Based on the previous work [14−16,18], the main mechanisms for the occurrence of serrated phenomenon mainly included two aspects, i.e. 1) dynamic strain ageing (DSA) and 2) the shearing of precipitates by dislocations. Following this, the heat treatment could be an effective way for suppressing the serrated flow occurred in Mg alloys. However, previous work mainly focused on the effect of heat treatment on the improvement of mechanical strength of Mg

* Corresponding author. Environmental Corrosion Center, Institute of Metal Research, Chinese Academy of Sciences, 62 Wencui Road, Shenyang 110016, China. Tel.: +86 24 23915897; fax: +86 24 23894149.
E-mail address: dkxu@imr.ac.cn (D.K. Xu).
Peer review under responsibility of National Engineering Research Center for Magnesium Alloys of China, Chongqing University.

http://dx.doi.org/10.1016/j.jma.2015.02.003.

alloys [8,13,22−25]. Regarding the serrated phenomenon and mechanical abnormity of the Mg−Li alloys at elevated temperature, few relevant literature can be referred.

In this work, the target is to investigate the PLC effect and the mechanical properties of the I-phase reinforced Mg−4% Li−6%Zn−1.2%Y alloy after extrusion, solid solution and ageing treatments. Through comparing the difference of the serrated flow, mechanical properties, fractography between different conditions tested at different temperatures, the effect of heat treatment and testing temperature on the mechanical abnormity and serrated phenomenon of the alloy will be explained.

2. Experimental procedures

The material investigated in this study is an as-extruded Mg−4%Li−6%Zn−1.2%Y (wt. %) alloy, which is prepared in the Magnesium Alloy Research Department of IMR, China. After holding at 300 °C for 2 h, the ingot was extruded into a plate with a dimension of 18 × 100 mm and an extrusion ratio of 5. Tensile samples with a gauge length of 25 mm, width of 4 mm and thickness of 3 mm were machined from the extruded plate. The axial direction of the tensile specimens was parallel to the extrusion direction. The stepped solid solution treatment of 330 °C/4h + 400 °C/1h + 450 °C/2h and subsequently aging treatment at 200 °C for 6 h were performed for some tensile samples. After that, tensile tests were conducted on a Multi-purpose testing machine with a constant strain rate of $1.33 \times 10^{-4}\ s^{-1}$ at room temperature, 100 °C and 200 °C. To ensure the reliability of the tensile data, three repeated tests were carried out for each condition. Phase analysis was conducted with a D/Max 2400 X-ray diffractometer (XRD) using monochromatic CuKα radiation, a step size of 0.02°and a scan rate for data acquisition of 4°/min. The microstructure and the fracture surfaces of differently heat-treated samples were observed by using scanning electron microscopy (SEM; XL30-FEG-ESEM).

3. Results and discussion

3.1. Microstructure

Fig. 1 shows the XRD pattern of differently heat-treated samples. It indicates that samples in the extruded and solution conditions are mainly composed of I-phase and α-Mg. After artificial ageing treatment, diffraction peaks associated with $MgZn_2$ phase emerges. Previous work reported that $MgZn_2$ phases can precipitate along the grain boundary and in the grain interior after ageing treatment [26−31]. Fig. 2 shows the microstructure of the Mg−4%Li−6%Zn−1.2%Y alloy. Generally, I-phase could form eutectic pockets with the α-Mg matrix in Mg−Li alloys [9]. After extrusion, the coarse I-phase/α-Mg eutectics are severely broken into tiny particles, as shown in Fig. 2 (a) and (b). After solution treatment, the extrusion streamlined microstructure is weakened, but a certain amount of smaller I-phase particles can be observed in the α-Mg matrix, as shown in Fig. 2 (c) and (d). Kim et al.

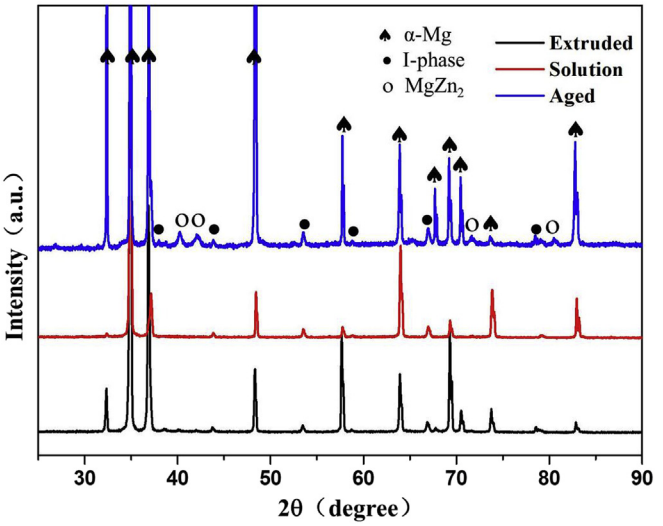

Fig. 1. XRD pattern of the Mg−4%Li−6%Zn−1.2%Y samples in three different heat treatment conditions.

reported that I-phase particles can precipitate from α-Mg matrix at temperatures ranging from 350 to 420 °C [32]. Therefore, the formation of these smaller I-phase particles in the solution treated samples is ascribed to the high temperature precipitation. After the subsequent ageing at 200 °C for 6 h, lots of $MgZn_2$ particles precipitate at the grain boundaries and in the grain interior, as shown in Fig. 2 (e) and (f).

3.2. Tensile properties

Stress-strain curves of differently heat-treated samples tested at different temperatures are shown in Figs. 3−5, respectively. It reveals that the curves are serrated after reaching a critical strain. In all conditions, both the yield strength ($\sigma_{0.2}$) and ultimate strength (σ_b) decrease with the temperature increasing. At elevated temperature, the work-hardening rate is close to zero or even a negative value, which is consistent with the results found in ZE41 and QE22 Mg alloys [33]. Fig. 3 shows that the serration is not well-distributed and its amplitude mainly varies from 3 to 6 MPa at room temperature, whereas the serrated amplitudes tested at 100 °C and 200 °C are mainly in the range of 0.2−0.4 MPa. Thus, it indicates that the pinning effect of solute atoms on dislocation movement decreases with the increasing of temperature. With the temperatures increasing, the yield strength ($\sigma_{0.2}$) and ultimate tensile strength (σ_b) are remarkably reduced, as listed in Table 1. Meanwhile, it reveals that the higher temperature is, the more strength decreases. However, the plasticity of the alloy increases with the increase of temperature and the elongation ratio can reach 45% at 200 °C. Fig. 4 shows that after solution treatment, all the serrations are well-distributed relatively and its amplitudes mainly vary between 0.2 and 0.3 MPa when tested at 100 °C and 200 °C. Similar to the as-extruded condition, the yield strength ($\sigma_{0.2}$) and ultimate tensile strength (σ_b) of the solubilized condition also decrease with the temperature increasing from 100 °C to 200 °C, as listed in Table 2.

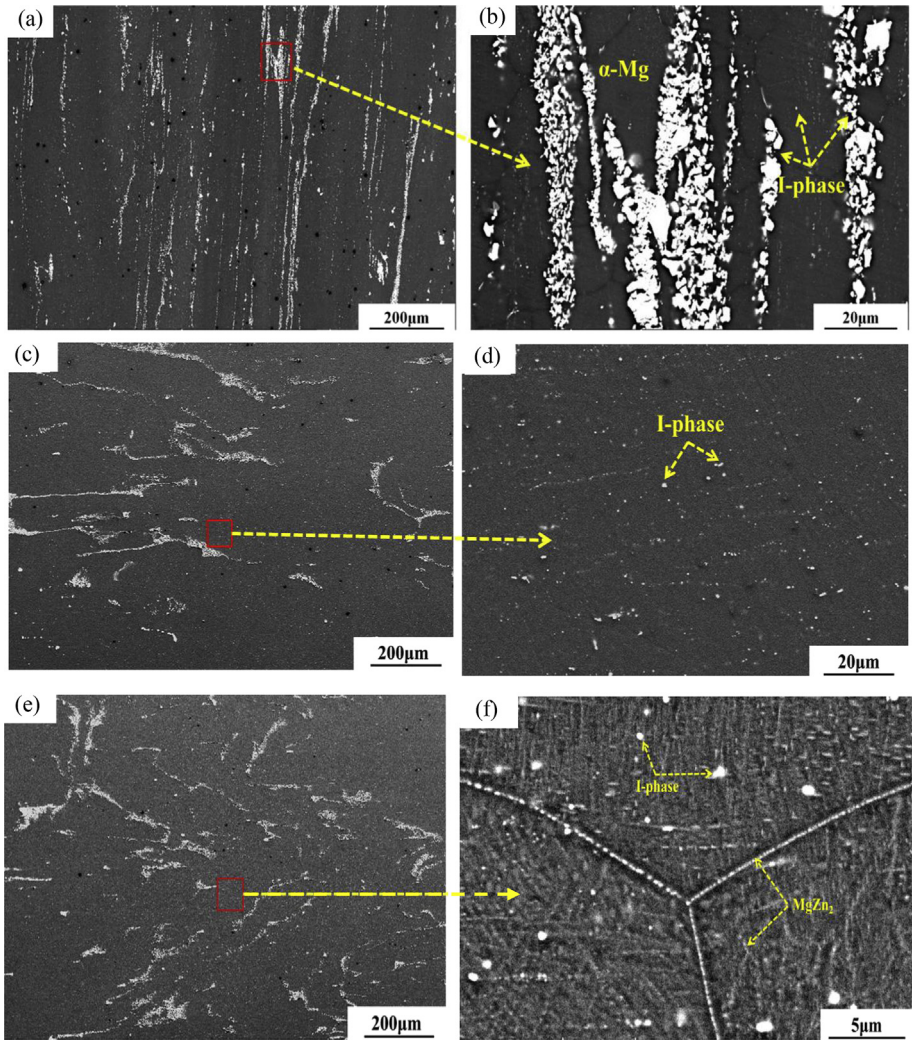

Fig. 2. Microstructure images of the differently heat treated Mg–4%Li–6%Zn–1.2%Y samples: (a) and (b) as-extruded, (c) and (d) solid solution treated, (e) and (f) age-treated. Images (b), (d) and (f) are the high magnified observations to the squared areas in images (a), (c) and (e), respectively.

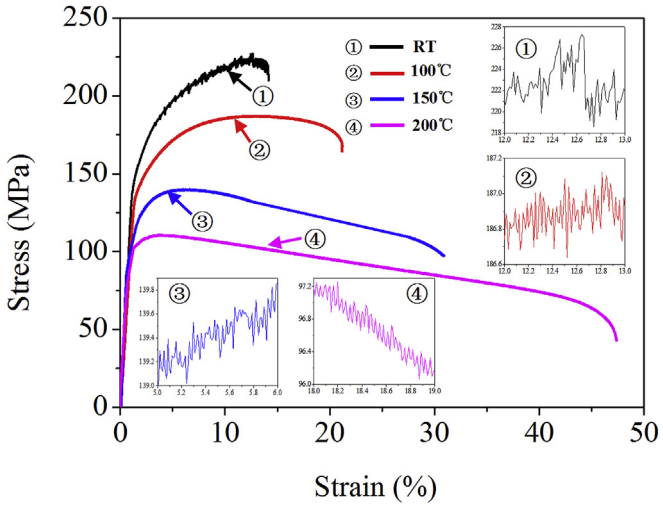

Fig. 3. Tensile curves of the as-extruded Mg–4%Li–6%Zn–1.2%Y samples tested at different temperatures.

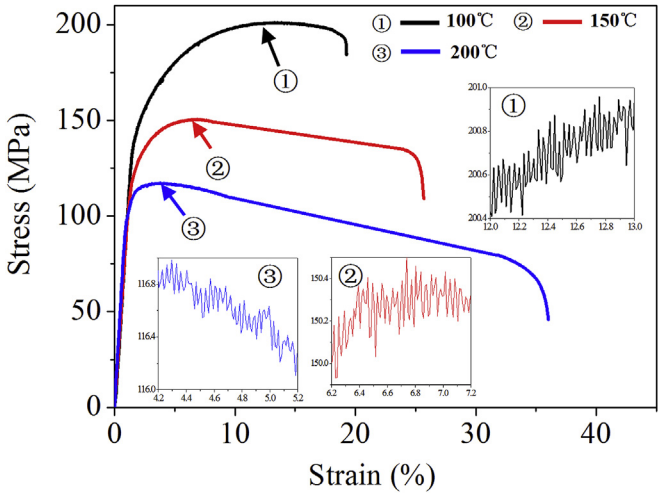

Fig. 4. Tensile curves of the solution treated Mg–4%Li–6%Zn–1.2%Y samples tested at different temperatures.

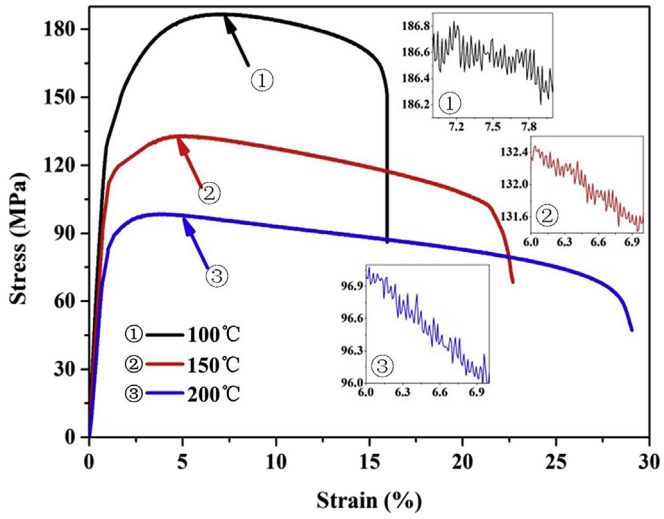

Fig. 5. Tensile curves of the as-extruded Mg−4%Li−6%Zn−1.2%Y samples after the solid solution and ageing treatment tested at different temperatures.

Table 1
The mechanical properties of the as-extruded Mg−4%Li−6%Zn−1.2%Y samples tested at different temperatures.

T (°C)	$\sigma_{0.2}$ (MPa)	σ_b (MPa)	δ (%)
RT	145	227	11
100	136	187	19
150	121	142	29
200	84	110	45

Fig. 5 shows that all the serrations are well-distributed for the aged samples tensile tested at 100 °C and 200 °C. The serration amplitude is mainly between 0.1 and 0.2 MPa, which is lower than that of samples in solution condition. It demonstrates that the pinning effect of solute atoms on dislocation movements is weaker than that of the solution treated samples. With the temperature increasing, the yield strength ($\sigma_{0.2}$) and ultimate tensile strength (σ_b) reduce from 132 MPa and 186 MPa to 88 MPa and 98 MPa, respectively, as listed in Table 3.

3.3. Fractography

Fig. 6 shows fracture surfaces of the Mg−4%Li−6%Zn−1.2%Y alloy under different heat treatment conditions tested at different temperatures. For the as-extruded condition, the quantity of plastic dimples increases with the temperature increasing, as shown in Fig. 6(b)−(d). It reveals that the plasticity of the alloy improves with temperature increasing.

Table 2
The mechanical properties of the solid solution treated Mg−4%Li−6%Zn−1.2%Y samples tested at different temperatures.

T (°C)	$\sigma_{0.2}$ (MPa)	σ_b (MPa)	δ (%)
100	140	201	11
150	119	150	22
200	99	117	34

Table 3
The mechanical properties of the solid solution plus age treated Mg−4%Li−6%Zn−1.2%Y samples tested at different temperatures.

T (°C)	$\sigma_{0.2}$ (MPa)	σ_b (MPa)	δ (%)
100	132	186	15
150	110	135	22
200	88	98	28

After solid solution treatment, the quantity of plastic dimples reduces obviously, as shown in Fig. 6(e)−(g). When tensile tested at 150 °C, the amount of dimples and their diameter in the solution treated samples are the least and some cleavage planes or steps emerge, demonstrating its poor plasticity. However, the amount of dimples tensile tested at 200 °C decreases slightly but their diameter increases obviously. Thus, the fracture mode of solution treated samples belongs to the ductile-brittle mixed fracture. Moreover, the fractions of ductile and brittle regions on fracture surfaces vary with the tensile testing temperature. For the samples in aged condition, a transformation from brittle fracture to ductile-brittle mixed fracture can be observed when the tensile testing temperature increases, as shown in Fig. 6(h)−(j). Thus, the fracture mode of aged samples belongs to the ductile-brittle mixed fracture. Moreover, the fractions of ductile and brittle regions on the fracture surfaces vary with the tensile testing temperature.

3.4. Discussion

For Mg−4%Li−6%Zn−1.2%Y alloy in all conditions, the strength decreases and the ductility improves with the increase of testing temperature. The main reasons are as follows: with temperature increasing, the activity of atoms is enhanced and the critical resolved shear stress of slip planes reduces, leading to the activation of non-basal slip systems and the improvement of deformation coordination capability [34,35]. Moreover, the cross slip of dislocations is expected to be the dominant deformation mechanism at elevated temperature [35]. Since the movement of the dislocations is easier, the work hardening effect can be remarkably reduced or even eliminated during the tensile testing at elevated temperature. In addition, due to the quick precipitation and the coarsening of the precipitates (Fig. 2(e) and (f)), the mechanical properties of the aged condition are the lowest when compared with those of the as-extruded and solution treated samples.

As for the PLC effect, it can occur for Mg−4%Li−6%Zn−1.2%Y alloy in all conditions because of the interaction of dislocations and solute atoms/second phase particles [15,18,36−39]. Since the movement rate of dislocations is close to the diffusion rate of solute atoms and dynamic strain aging can easily occur [39], the PLC effect of the as-extruded samples is much remarkable at room temperature (in Fig. 3).Generally, the PLC effect of Mg alloys usually occurs at low temperature range [36−38]. Even at −25°Cand −50 °C, Mg-14.3Li-0.8Zn alloy can still present an obvious serrated flowing phenomenon [38]. With the temperature increasing, the PLC effect is remarkably reduced and only

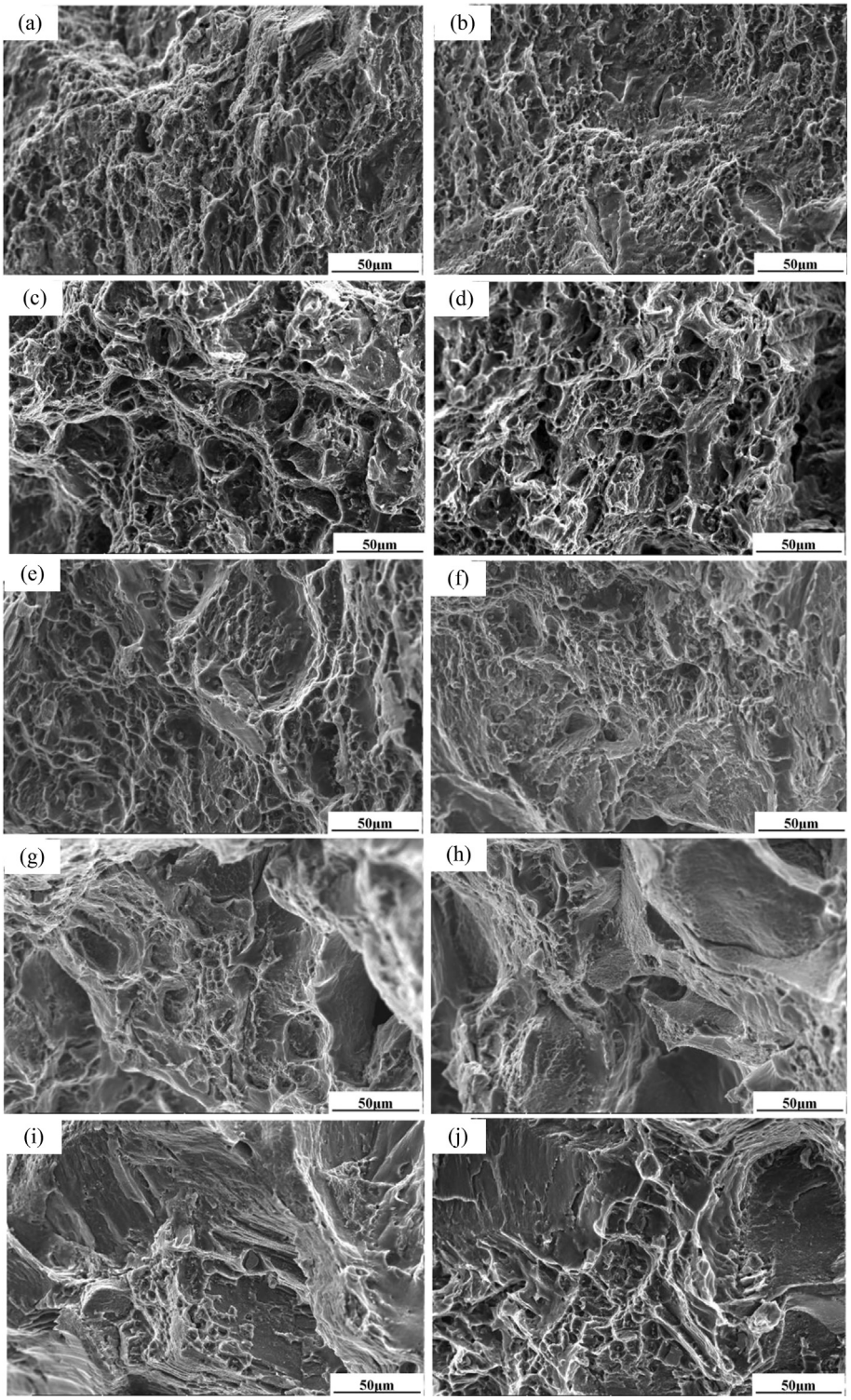

Fig. 6. Secondary electron images to the fracture surfaces of Mg–4%Li–6%Zn–1.2%Y samples tensile tested at different temperatures: (a)–(d) as-extruded, (e)–(g) solid solution treated, (h)–(j) age-treated; (a) room temperature, (b), (e) and (h) 100 °C, (c), (f) and (i) 150 °C, (d), (g) and (j) 200 °C.

feeble serrated amplitude can be observed (in Fig. 3), which can be ascribed to the weak interaction between dislocations and solute atoms because of much difference of movement speed between dislocations and solute atoms. For the solution treated samples, the mechanism of PLC effect is similar to that of the as-extruded samples. For the aged samples, $MgZn_2$ precipitates can act as the obstacle for impeding the movement of dislocations. With the strain increasing, the pile-up dislocations will cut through the precipitates and the stress drops suddenly [37]. Due to abundant $MgZn_2$ phase particles in matrix (in Fig. 2(f)), and the space between particles is small. Thus, the dislocations can be pinned again by the adjacent

particles after cutting the prior particles and then repeat the progress until fracture, showing an abnormal serrated flowing in the stress−strain curves. However, the serrated amplitude of the aged samples is the smallest when compared with the other two conditions, which can be mainly ascribed to the weak pining effect of the coarse precipitates on dislocation movement and less solute atoms in the matrix for influencing the pining and release of the pile-up dislocations.

4. Conclusions

1. During the tensile testing at elevated temperature, the Mg−4%Li−6%Zn−1.2%Y alloy has small serrated amplitude of less than 1 MPa, no matter it is in the conditions of the extrusion, solution or ageing treatment. The temperature increase can weaken the serrated amplitude but it cannot eliminate the PLC effect completely.
2. By comparing serrated flow of the alloys on different conditions, the serrated amplitude of the aged alloy is lowest and the value is only 0.1−0.2 MPa. The underlying mechanism for the plastic instability at the higher temperature (≥100 °C) can be ascribed to the weak pining effect of solute atoms on the movement of dislocation and easy release of the pile-up of dislocations.
3. The strength and the plasticity of the alloy are related with the temperature and heat treatment conditions. Meanwhile, an artificial ageing treatment can weaken the serrated phenomenon of Mg−4%Li−6%Zn−1.2%Y alloy.

Acknowledgments

This work was supported by the National Natural Science Foundation of China projects under Grant Nos. 51171192, 51271183 and 51301172, the National Basic Research Program of China (973 Program) project under Grant No. 2013CB632205 and the Innovation Fund of Institute of Metal Research (IMR), Chinese Academy of Sciences.

References

[1] J.M. Song, T.X. Wen, J.Y. Wang, Scr. Mater. 56 (2007) 529−532.
[2] Y. Froes, D. Eliezer, E. Aghion, JOM 5 (1998) 30−34.
[3] A.M. Russell, L.S. Chumbley, V.B. Gantovnik, Scr. Mater. 39 (1998) 1663−1667.
[4] H.W. Dong, F.S. Pan, B. Jiang, Y. Zeng, Mater. Des. 57 (2014) 121−127.
[5] C.H. Zhang, M.L. Zhang, L.L. Gao, R.Z. Wu, Mater. Lett. 62 (2008) 2177−2180.
[6] Y.W. Song, D.Y. Shan, R.S. Chen, E.H. Han, Corros. Sci. 51 (2009) 1087−1094.
[7] Y. Zeng, B. Jiang, D.H. Huang, J.H. Dai, F.S. Pan, J. Magnes. Alloy 1 (2013) 297−302.
[8] L. Bao, Q.C. Le, Z.Q. Zhang, J.Z. Cui, Q.X. Li, J. Magnes. Alloy 1 (2013) 139−144.
[9] D.K. Xu, T.T. Zu, M. Yin, Y.B. Xu, E.H. Han, J. Alloys Compd. 582 (2014) 161−166.
[10] D.K. Xu, E.H. Han, Prog. Nat. Sci. Mater. Inter 22 (2012) 364−385.
[11] D.K. Xu, E.H. Han, Scr. Mater. 71 (2014) 21−24.
[12] H. Takuda, S. Kikuchi, N. Yoshida, H. Okahara, Mater. Trans. 11 (2003) 2266−2270.
[13] L. Zhang, J.H. Zhang, C. Xu, S.J. Liu, Y.F. Jiao, L.J. Xu, Y.B. Wang, J. Meng, R.Z. Wu, M.L. Zhang, Mater. Des. 61 (2014) 168−176.
[14] H.F. Jiang, Q.C. Zhang, X.D. Chen, Z.J. Chen, Z.Y. Jiang, X.P. Wu, J.H. Fan, Acta Mater. 55 (2007) 2219−2228.
[15] C. Wang, Y.B. Xu, E.H. Han, Mater. Lett. 60 (2006) 2941−2944.
[16] C. Wang, Z.Q. Li, Y.B. Xu, E.H. Han, J. Mater.Sci. 42 (2007) 3573−3579.
[17] P.T. Cao, Acta.Phy. Sinca 58 (2009) 5591−5597.
[18] Q. Hu, Q.C. Zhang, S.H. Fu, P.T. Cao, M.Gong, Theor. Appl. Mech. Lett. 1 011007 (2011).
[19] G.Y. Sha, T. Liu, T. Yu, H. Wang, Proc. Eng. 27 (2012) 1216−1221.
[20] T.Q. Li, Y.B. Liu, Z.Y. Cao, D.M. Jiang, L.R. Cheng, Mater. Sci. Eng. A 527 (2010) 7808−7811.
[21] V. Kumar, A. Gupta, D. Lahiri, K. Balani, J. Phys D: Appl. Phys. 46 (2013) 1−8.
[22] J.H. Zhang, L. Zhang, Z. Leng, S.J. Liu, R.Z. Wu, M.L. Zhang, Scr. Mater. 68 (2013) 675−678.
[23] X.H. Chen, X.W. Huang, F.S. Pan, A.T. Tang, J.F. Wang, D.F. Zhang, Trans. Nonferrous Met. Soc. China 21 (2011) 754−760.
[24] X.Y. Guo, R.Z. Wu, J.H. Zhang, B. Liu, M.L. Zhang, Mater. Des. 53 (2014) 528−533.
[25] G.H. Zhang, J.H. Chen, H.G. Yan, B. Su, X. He, M. Ran, J. Alloys Compd. 592 (2014) 250−257.
[26] B.C. Wei, C.Q. Chen, Z. Huang, Y.G. Zhang, Mater. Sci. Eng. A 280 (2000) 161−167.
[27] C.L. Mendis, K. Oh-ishi, T. Ohkubo, K. Hono, Mater. Sci. Eng. A 535 (2012) 122−128.
[28] C.L. Mendis, K. Oh-ishi, K. Hono, Scr. Mater. 57 (2007) 485−488.
[29] J. Buha, Mater. Sci. Eng. A 492 (2008) 11−19.
[30] X. Gao, J.F. Nie, Scr. Mater. 56 (2007) 645−648.
[31] Y. Lu, A.R. Bradshaw, Y.L. Chiu, I.P. Jones, J. Alloys Compd. 614 (2014) 345−352.
[32] I.J. Kim, D.H. Bae, D.H. Kim, Mat. Sci. Eng. A 359 (2003) 313−318.
[33] P. Lukac, Z. Trojanova, Mater. Sci. Eng. A 462 (2007) 23−28.
[34] C.M. Cepeda-Jimenez, J.M. Molina-Aldareguia, F. Carrenob, M.T. Perez-Prado, Acta Mater. 85 (2015) 1−13.
[35] Z. Drozd, Z. Trojanová, S. Kúdela, J. Alloys Compd. 378 (2004) 192−195.
[36] S.M. Zhu, J.F. Nie, Scr. Mater. 50 (2004) 51−55.
[37] D. Wu, R.S. Chen, E.H. Han, Mater. Sci. Eng. A 532 (2012) 267−274.
[38] S.K. Wu, C. Chien, C.S. Yang, H.Y. Bor, Mater. Sci. Eng. A 605 (2014) 33−38.
[39] C. Wang, Y.B. Xu, E.H. Han, Acta Metall. Sin. 42 (2006) 191−194.